

17,11

Structure formation processes in fullerene mixtures

© R.M. Khusnutdinoff^{1,2}, R.R. Khairullina¹

¹Kazan Federal University,
Kazan, Russia

²Udmurt Federal Research Center, Ural Branch Russian Academy of Sciences,
Izhevsk, Russia

E-mail: khrm@mail.ru

Received October 17, 2022

Revised October 24, 2022

Accepted October 25, 2022

Glass formation processes in condensed matter are characterized by some specific short-range order changes in the arrangement of particles (atoms/molecules/ions). So, the short-range structural order in supercooled liquids and glasses is characterized by fivefold symmetry in the arrangement of particles, often referred to as icosahedral (ideal or distorted) short-range order. This article is devoted to the study of local structural features of the supercooled melt of the $A_{20}B_{80}$ fullerene mixture (where $A = C_{60}$ and $B = C_{70}$) obtained under various cooling protocols in order to elucidate the mechanism of formation of the icosahedral short-range order in binary molecular liquids. Comprehensive studies of the properties of a fullerene mixture melt were carried out using large-scale molecular dynamics simulations followed by structural and cluster analysis. The crystallization temperature and the critical glass transition temperature of the system were calculated to be $T_m \approx 1439$ K and $T_c \approx 1238$ K, respectively. It has been established that the crystallization of a binary fullerene mixture proceeds according to the polycrystalline scenario with the formation of clusters with fcc and hcp symmetries. It is shown that in a supercooled fullerene mixture, the short-range icosahedral order is formed by an insignificant number of ideal icosahedral clusters and a certain set of distorted icosahedral clusters, the fraction of which remains practically unchanged at temperatures below the critical glass transition temperature.

Keywords: molecular dynamics, fullerenes, short-range order, structural ordering.

DOI: 10.21883/PSS.2023.01.54991.501

1. Introduction

The near structural order in supercooled liquids and glasses is characterized by a number of specific features and a complex set of correlation lengths [1]. Recent molecular dynamics studies have shown the presence of so-called distorted icosahedral structures in the supercooled melt phase in various classes of liquids (pure transition metals, multicomponent metal melts, molecular liquids) [2–5]. The short-range structural order of such systems is of scientific interest, since it is believed that the local structure of melts has a strong influence on its microscopic collective dynamics, viscoelastic and transport properties, as well as the glass-forming ability of the substance [6,7].

According to Frank's idea [8], the near icosahedral order should be energetically advantageous for systems in the supercooled melt phase. Despite the fact that this idea has been around for more than half a century, there is still no direct experimental information about the near structural order prevailing in supercooled liquids. The icosahedral short-range order in supercooled liquids and amorphous alloys is indirectly detected in neutron and X-ray diffraction experiments [2,3]. Thus, the presence of shoulders and widenings at the second maximum in the experimentally measured value — in the static structure factor $S(k)$ — is usually interpreted as a manifestation of the icosahedral

(ideal or distorted) short-range order. The experimentally obtained structure factors are modeled under the assumption that the liquid consists of clusters with different short-range structures. In the case of supercooled liquids, the best correspondence to experimental data is obtained if it is assumed that there are structures with fivefold symmetry in the arrangement of particles (atoms/molecules/ions) in the system — icosahedral clusters. At the same time, spectroscopy experiments involving inelastic scattering of neutrons and X-rays, Raman scattering of light, may contain only indirect information about the presence of icosahedral clusters in the [9,10] system. Thus, in order to identify the short-range structural order in a substance, additional methods of interpretation of experimental scattering spectra are required. Such, for example, include microscopic theories of structural relaxation of particle number density fluctuations the mode-coupling theory self-consistent relaxation theory and others, where the parameters of the theories are interrelated with the structural characteristics of the system [11–14]. Another alternative in determining the structural features of disordered systems are the methods of classical and quantum mechanical (first-principle) molecular dynamic simulation, which together with the methods of structural and cluster analysis allow us to describe in detail the processes of structure formation in such systems.

The purpose of this work is to study the local structural features of the equilibrium and supercooled melt of a fullerene mixture $A_{20}B_{80}$ (where $A=C_{60}$ and $B=C_{70}$), obtained with various cooling protocols in order to elucidate the mechanism of formation of icosahedral short-range order in binary molecular fluids.

2. Modeling details and methods used

A system consisting of 32 000 molecules (6400 and 25 600 fullerene molecules C_{60} and C_{70} , respectively) located in a cubic cell with periodic boundary conditions is considered. The interaction between the molecules is determined by the effective short-range potential of the intermolecular interaction of the spherical type — the Girifalco potential [15–18]. Physical quantities are measured in potential parameters as presented in Ref. [19]. Molecular dynamic calculations were performed in an NpT ensemble at a pressure of $p^* = 0.07$ ($p = 3.5$ MPa) in the temperature range $T^* = [0.05–0.650]$ ($T = [154.7–2011]$ K). The cooling rates of the systems were $\gamma^* = 0.000016$, 0.00016 and 0.0016 ($\gamma = 10^{10}$, 10^{11} and 10^{12} K/s). The integration of the equations of motion of molecules was performed using the velocity Verlet algorithm with a time step $\tau^* = 0.001$ ($\tau = 5.0$ fs). To bring the system into a state of thermodynamic equilibrium, the program performed 10^5 time steps and $2 \cdot 10^6$ steps to calculate structural characteristics and distribution functions, as well as to perform cluster analysis.

3. Results and discussion

To identify the process of glass formation in the melt of a fullerene mixture, the temperature dependence of the potential energy of the system obtained with various cooling protocols was calculated. In particular, the cooling of the equilibrium melt of a mixture of fullerenes was carried out at cooling rates: $\gamma = 10^{10}$, 10^{11} and 10^{12} K/s. The left column of Fig. 1, *a* shows the temperature dependence of the potential energy per molecule at different cooling rates. At $\gamma = 10^{10}$ K/s in the vicinity of the temperature $T^* = 0.465$ ($T_m \approx 1439$ K), the values of $U(T)$ demonstrate sharp changes that indicate a phase transition „liquid–crystal“. At the same time, at the cooling rate of $\gamma = 10^{11}$ K/s below the melting point, the system is in the metastable phase of the supercooled melt, which, upon subsequent cooling, turns into a crystalline state. At a sufficiently high cooling rate $\gamma = 10^{12}$ K/s there is a monotonous change in the energy slope with temperature, which demonstrates the characteristics with the kinetic „liquid–glass“ transition. To determine the critical glass transition temperature, the

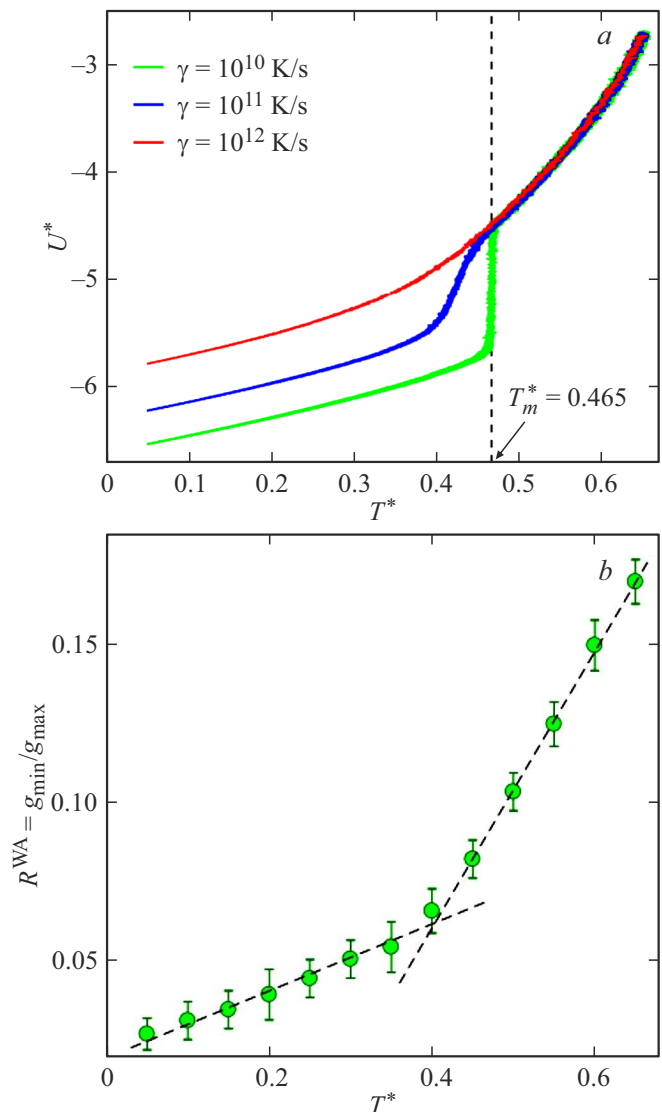


Figure 1. *a* — the potential energy of a fullerene mixture per molecule as a function of temperature at different cooling rates, *b* — temperature dependence of the Wendt–Abraham order parameter. The intersection of the interpolation lines determines the critical glass transition temperature of the system.

Wendt–Abraham order parameter was calculated

$$R^{WA} = g_{min}/g_{max}, \quad (1)$$

where g_{min} and g_{max} are the values of the first minimum and maximum in the radial distribution function of molecules, respectively. The right column of Fig. 1, *b* shows the temperature dependence of the Wendt–Abraham order parameter, by the intersection of the interpolation lines of which the critical glass transition temperature $T_c^* = 0.40 \pm 0.01$ ($T_c \approx 1238$ K) was determined. We note that the critical glass transition temperature is approximately 20% higher than the glass transition temperature. The estimated value of the glass transition temperature shows the correct

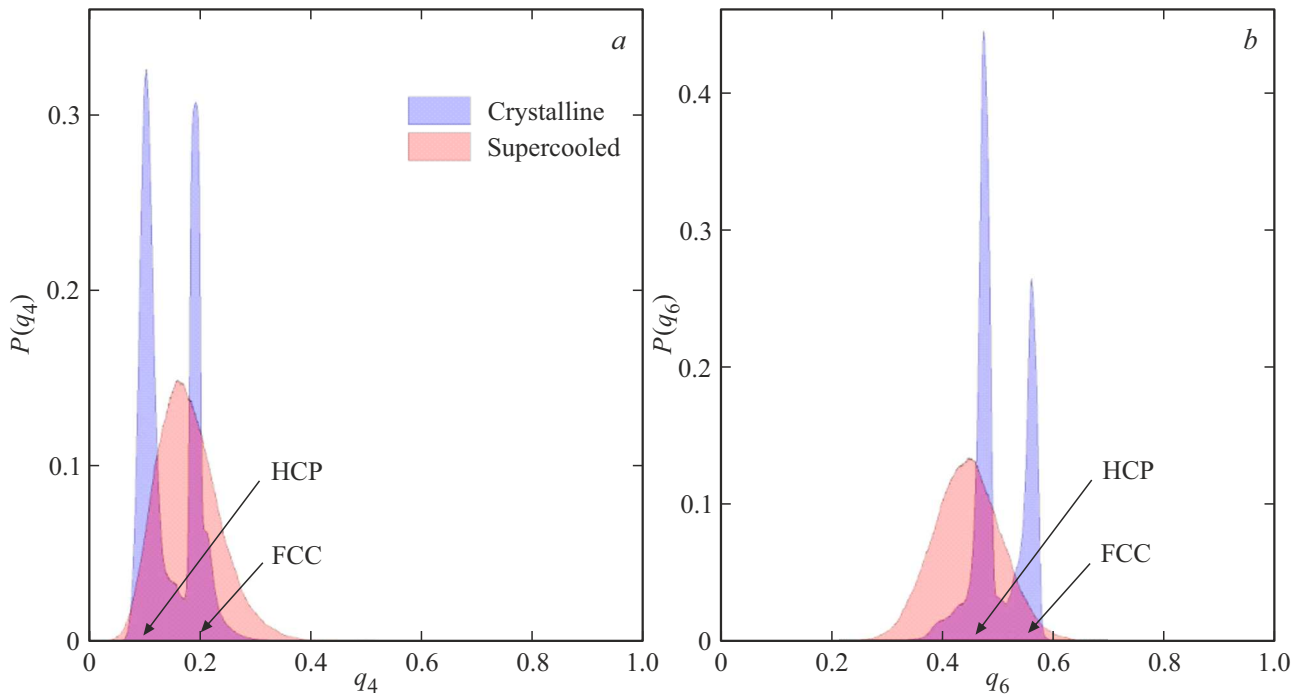


Figure 2. Distribution functions $P(q_4)$ and $P(q_6)$ for a supercooled and crystalline fullerene mixture at a temperature of $T^* = 0.400$. It can be seen that the crystallization of a mixture of fullerenes is carried out according to a polycrystalline scenario with the formation of two types of crystal clusters: face-centered cubic (FCC) and hexagonal closed packed (HCP) crystal structures (see Table 1).

implementation of the 2/3 rule for the ratio between T_g and T_m ($T_g^*/T_m^* = 0.688$) [20].

To identify local structural features in a supercooled fullerene mixture, we use the method of cluster analysis based on rotational invariants [21–24]. In the framework of this approach, for each i - of that particle, the number of nearest neighbors of $N_b(i)$ is determined. The vectors \mathbf{r}_{ij} connecting the i -particle with its nearest neighbors ($j = 1, N_b$) allow us to determine the local orientation parameter $q_{lm}(i)$ for each particle

$$g_{lm}(i) = \frac{1}{N_b(i)} \sum_{j=1}^{N_b(i)} Y_{lm}(\theta_j, \varphi_j), \quad (2)$$

where $Y_{lm}(\theta, \varphi)$ there are spherical harmonics, (θ, φ) — angular coordinates j - of that particle, defined by the vector \mathbf{r}_{ij} . We note that the local orientation order determined in this way depends only on two parameters — the angular distribution of the nearest neighbors θ_i and φ_i ; in this case, all particles located within the first coordination sphere are neighbors. For each particle, rotational invariants of the second kind are calculated $q_l(i)$:

$$q_l(i) = \sqrt{\frac{4\pi}{(2l+1)} \sum_{m=-l}^{m=l} |q_{lm}(i)|^2}. \quad (3)$$

It is important to note that each type of crystal lattice is characterized by a unique set of rotation invariants q_l . Thus, by comparing the values q_l calculated for each particle with

Table 1. Local orientation order parameters for face-centered cubic (FCC), hexagonal closed packed (HCP), simple cubic (SC), body-centered cubic (BCC) and icosahedral (ICO) crystal structures

Crystal Symmetry	q_4	q_6
FCC	0.190	0.574
HCP	0.097	0.484
SC	0.763	0.353
BCC	0.082	0.500
ICO	0	0.663

the values q_l^{id} for ideal lattices, it is possible to determine the presence of ordered structures. To identify the crystal structure, rotational invariants of the second kind (q_4, q_6) are usually used, which are easily calculated for ideal crystals. These invariants for different types of lattices are given in Table 1. For a liquid, the values of the presented parameters are close to zero.

Fig. 2 shows the distributions of $P(q_4)$ and $P(q_6)$ for a supercooled and crystalline fullerene mixture at a temperature of $T^* = 0.400$. As can be seen from the figure, based on the presented cluster analysis, supercooled melts of the fullerene mixture do not contain ideal or distorted clusters with icosahedral (fivefold) symmetry. Thus, cluster

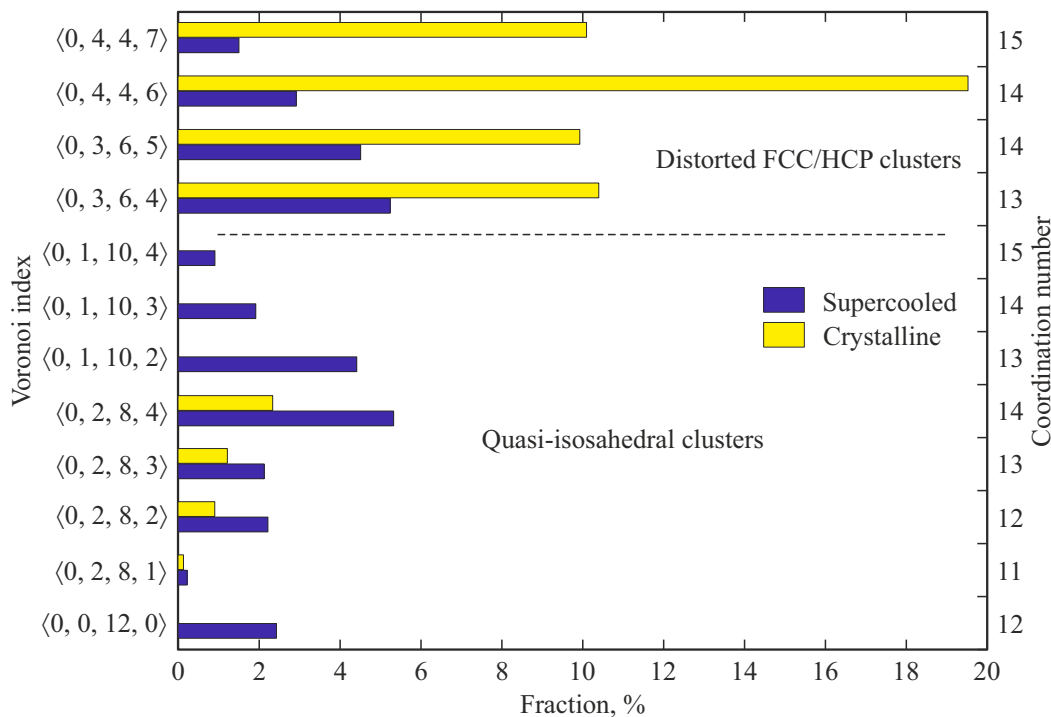


Figure 3. Distribution of the main Voronoi clusters in a supercooled and crystalline fullerene mixture at a temperature $T^* = 0.400$. The proportion of distorted ICO clusters in a supercooled solution of a mixture of fullerenes $A_{20}B_{80}$ (where $A = C_{60}$ and $B = C_{70}$) is $\eta = 19.4\%$. While in the crystalline phase, they are not more than 4.5% .

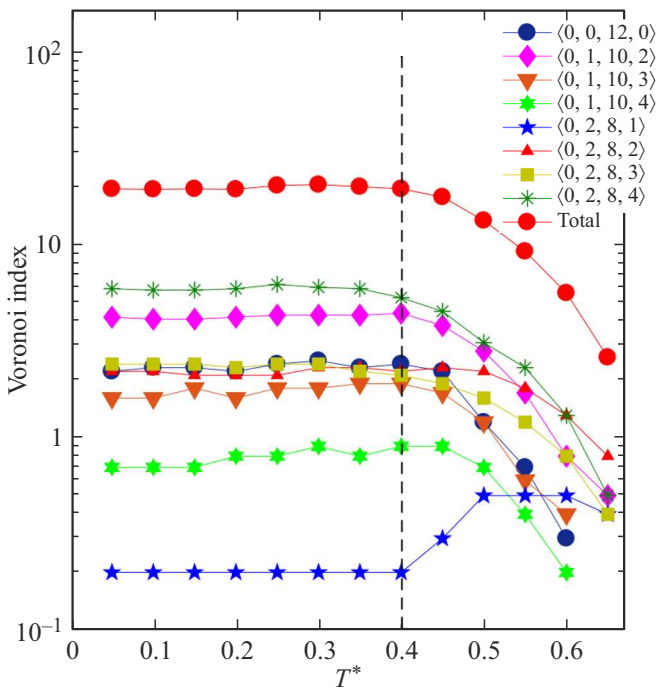
analysis based on the rotational invariants q_4 and q_6 does not reveal any evidence of the presence of an icosahedral short-range order in a supercooled melt of a mixture of fullerenes. At the same time, the crystallization of the fullerene mixture at sufficiently high cooling rates ($\gamma = [10^{10}, 10^{11}]$ K/s) proceeds according to a polycrystalline scenario with the formation of clusters with FCC and HCP symmetries. The percentage composition of crystallites is $f_{\text{FCC}} \approx 26\%$ and $f_{\text{HCP}} \approx 23\%$.

A detailed short-range analysis in liquids was performed using the Voronoi polyhedron method [25,26]. The Voronoi polyhedron is described by the indices (n_3, n_4, n_5, n_6) , where n_i denotes the number of faces with i edges, and the sum of the values of n_i determines the coordination number of the system, i.e. $z = \sum_i n_i$. For example, the Voronoi index $\langle 0, 0, 12, 0 \rangle$ denotes an ideal ICO cluster with fivefold symmetry, while clusters with indices $\langle 0, 1, 10, x \rangle$, $\langle 0, 2, 8, x \rangle$, (where $x = 1, 2, 3, 4$) it can be considered as distorted ICO clusters. Clusters with BCC symmetry are characterized by the index $\langle 0, 6, 0, 8 \rangle$. The Voronoi index $\langle 0, 0, 12, 2 \rangle$ denotes a 14-coordinated atom, and $\langle 0, 0, 12, 2 \rangle$ characterizes a tetragonal close-packed structure of the Frank–Casper type. At the same time, the traditional Voronoi method cannot distinguish between ideal or almost ideal crystal structures with FCC and HCP symmetries. For example, FCC/HCP clusters have the index $\langle 0, 12, 0, 0 \rangle$. Voronoi indices for various types of crystal symmetry are given in Table 2.

For the purpose of a detailed study of the short-range order in a mixture of fullerenes, the distribution of the main types of clusters is analyzed. Fig. 3 shows the content of Voronoi clusters in the supercooled and crystalline phases of a mixture of fullerenes $A_{20}B_{80}$ (where $A = C_{60}$ and $B = C_{70}$) at a temperature of $T^* = 0.400$. As can be seen from the figure, in the supercooled and crystalline phases of the fullerene mixture, a number of distorted icosahedral clusters are observed, which were not detected earlier in the framework of the rotational invariant method. In the supercooled melt, the near icosahedral order is formed by an insignificant number of ideal icosahedral clusters ($\sim 2.4\%$) and some set of distorted icosahedral clusters ($\sim 17\%$), denoted by Voronoi indices: $\langle 0, 1, 10, x \rangle$ and $\langle 0, 2, 8, x \rangle$, where $x = 1, 2, 3$ and 4 . At the same time, distorted clusters with FCC and HCP symmetries are detected in the system. The share of such clusters is about 14% . It should be noted that the above indices demonstrate the presence of icosahedron fragments in the systems under consideration. Such formation of icosahedral structures in melts is denoted by the term icosahedral ordering, which is often used to describe the local topological short-range order in supercooled liquids and glasses [3]. The structure of the fullerene mixture in the crystalline phase is mainly formed by distorted FCC/HCP clusters ($\sim 50\%$) and quasi-icosahedral clusters ($\sim 4.3\%$), denoted by Voronoi indices: $\langle 0, 2, 8, x \rangle$, where $x = 1, 2, 3$ and 4 . It should be noted that the transition „liquid–crystal“ in a fullerene mixture is

Table 2. Voronoi indices for various types of crystal symmetries

Crystal symmetry	Indexes Voronoi	Comments
FCC	$\langle 0, 12, 0, 0 \rangle$	Ideal FCC polyhedron
	$\langle 0, 3, 6, 4 \rangle$	Distorted FCC polyhedron
	$\langle 0, 3, 6, 5 \rangle$	Distorted FCC polyhedron
	$\langle 0, 4, 4, 6 \rangle$	Distorted FCC polyhedron
	$\langle 0, 4, 4, 7 \rangle$	Distorted FCC polyhedron
HCP	$\langle 0, 12, 0, 0 \rangle$	Ideal HCP polyhedron
BCC	$\langle 0, 6, 0, 8 \rangle$	Ideal BCC polyhedron
ICO	$\langle 0, 0, 12, 0 \rangle$	Ideal ICO polyhedron
	$\langle 0, 1, 10, x \rangle$, $x = 1, 2, 3, 4$	Distorted ICO-polyhedron
	$\langle 0, 2, 8, x \rangle$, $x = 1, 2, 3, 4$	Distorted ICO-polyhedron
TCP	$\langle 0, 0, 12, 2 \rangle$	Tetragonal close-packed Frank–Casper Structure

**Figure 4.** Temperature dependence of the distribution of icosahedral clusters in a fullerene mixture.

accompanied by the transformation of distorted icosahedral clusters into clusters with FCC/HCP symmetries.

Figure 4 shows the temperature dependence of the distribution of icosahedral clusters in a fullerene mixture, determined by Voronoi indices during cooling of the system at a rate of $\gamma = 10^{12}$ K/s. It can be seen from the figure that

with a decrease in temperature, an increase in the number of molecular formations with ideal and distorted fivefold symmetry is observed. At temperatures below the critical glass transition temperature, the proportion of icosahedral clusters in the system practically does not change. The only exceptions are polyhedra defined by the indices $\langle 0, 1, 10, 1 \rangle$ (not represented in figure) and $\langle 0, 2, 8, 1 \rangle$. The former, due to the specific features of the intermolecular interaction of fullerenes (short-range, absence of the oscillating part, etc.), are not formed in the system [27]. At the same time, the proportion of molecular formations determined by the Voronoi indices $\langle 0, 2, 8, 1 \rangle$ decreases to the critical glass transition temperature T_c^* and reaches a plateau at temperatures below T_c^* .

4. Conclusion

This paper presents the results of molecular dynamics simulation of a fullerene mixture $A_{20}B_{80}$ (where $A = C_{60}$ and $B = C_{70}$) for a wide range of temperature values. The crystallization temperature and critical glass transition temperature of the system were determined, which were $T_m \approx 1439$ K and $T_c \approx 1238$ K, respectively. It is established that the crystallization of a fullerene mixture, at sufficiently high cooling rates ($\gamma = [10^{10}, 10^{11}]$ K/s), proceeds according to a polycrystalline scenario with the formation of clusters with FCC- and HCP-symmetries.

It was found that in a supercooled fullerene mixture $A_{20}B_{80}$ (where $A = C_{60}$ and $B = C_{70}$) the near icosahedral order is formed by an insignificant number of ideal icosahedral clusters ($\sim 2.4\%$) and some set of distorted icosahedral clusters ($\sim 17\%$). It is shown that at temperatures below

the critical glass transition temperature, the proportion of icosahedral clusters in the system practically does not change.

Funding

The work is supported by the Russian Scientific Foundation (project No. 22-22-00508).

Large-scale molecular dynamic calculations were performed using the equipment of the Center for Collective Use of Ultra-High-performance Computing Resources of Lomonosov Moscow State University and on the computing cluster of Kazan (Volga Region) Federal University.

Conflict of interest

The authors declare that they have no conflict of interest.

References

- [1] A.V. Mokshin, R.M. Khusnutdinoff, B.N. Galimzyanov, V.V. Brazhkin. *Phys. Chem. Chem. Phys.* **22**, 4122 (2020).
- [2] W.K. Luo, H.W. Sheng, F.M. Alamgir, J.M. Bai, J.H. He, E. Ma. *Phys. Rev. Lett.* **92**, 145502 (2004).
- [3] T. Schenk, D. Holland-Moritz, V. Simonet, R. Bellissent, D.M. Herlach. *Phys. Rev. Lett.* **89**, 075507 (2002).
- [4] R.M. Khusnutdinoff, A.V. Mokshin, B.A. Klumov, R.E. Ryltsev, N.M. Chtchelkatchev. *J. Exp. Theor. Phys.* **123**, 265 (2016).
- [5] L. Ren, T. Gao, R. Ma, Q. Xie, X. Hu. *Mater. Res. Express* **6**, 016510 (2019).
- [6] R.M. Khusnutdinoff, A.V. Mokshin. *Solid State Phenom.* **310**, 145 (2020).
- [7] R.M. Khusnutdinoff, R.R. Khairullina, A.L. Beltyukov, V.I. Lad'yanov, A.V. Mokshin. *J. Phys.: Condens. Matter.* **33**, 104006 (2021).
- [8] F.C. Frank. *Proc. R. Soc. London A* **215**, 43 (1952).
- [9] P. Zimmermann, S. Peredkov, P. Macarena Abdala, S. DeBeer, M. Tromp, C. Müller J.A. van Bokhoven. *Coord. Chem. Rev.* **423**, 213466 (2020).
- [10] J.B. Kimbrell, C.M. Crittenden, W.J. Steward, F.A. Khan, A.C. Gaquere-Parker, D.A. Stuart. *Nanosci. Meth.* **3**, 40 (2014).
- [11] W. Götzke. *Complex dynamics of glass-forming liquids*. Oxford University Press, Oxford (2009). 1937 p.
- [12] J.P. Hansen, I.R. McDonald. *Theory of simple liquids*. Academic Press, London (1986). 416 p.
- [13] A.V. Mokshin. *Theor. Math. Phys.* **183**, 449 (2015).
- [14] R.M. Khusnutdinoff, A.V. Mokshin, A.L. Bel'tyukov, N.V. Olyanina. *High Temp.* **56**, 201 (2018).
- [15] L.A. Girifalco. *J. Chem. Phys.* **95**, 5370 (1991).
- [16] K. Kniáz, J.E. Fischer, L.A. Girifalco, A.R. McGhie, R.M. Strongin, A.B. Smith. *Solid State Commun.* **96**, 739 (1995).
- [17] V.I. Zubov, I.V. Zubov. *J. Phys. Chem. B* **109**, 14627 (2005).
- [18] R. Ruberto, M.C. Abramo, C. Caccamo. *Phys. Rev. B* **70**, 155413 (2004).
- [19] R.M. Khusnutdinoff, A.V. Mokshin, I.D. Takhaviev. *Phys. Solid State* **57**, 412 (2015).
- [20] V.K. Malinovskii. *Phys. Solid State* **41**, 725 (1999).
- [21] P.R. ten Wolde, M.J. Ruiz-Montero, D. Frenkel. *J. Chem. Phys.* **104**, 9932 (1996).
- [22] S. Torquato, T.M. Truskett, P.G. Debenedetti. *Phys. Rev. Lett.* **84**, 2064 (2000).
- [23] J.R. Errington, P.G. Debenedetti. *J. Chem. Phys.* **118**, 2256 (2003).
- [24] B.A. Klumov, S.A. Khrapak, G.E. Morfill. *Phys. Rev. B* **83**, 184105 (2011).
- [25] C.C. Wang, K.J. Dong, A.B. Yu. *AIP Conf. Proc.* **1542**, 353 (2013).
- [26] S.-P. Pan, S.-D. Feng, J.-W. Qiao, W.-M. Wang, J.-Y. Qin. *Sci. Rep.* **5**, 16956 (2015).
- [27] M.B. Yunusov, R.M. Khusnutdinoff, A.V. Mokshin. *Phys. Solid State* **63**, 372 (2021).